Modulation of stretch reflexes to environmental dynamics and perturbation properties

Alejandro del Valle Hidalgo

TU Delft

Modulation of stretch reflexes to environmental dynamics and perturbation properties

by

A. del Valle Hidalgo

to obtain the degree of Master of Science in Biomedical Engineering
at the Delft University of Technology,
to be defended publicly on Friday September 27, 2019.

Student number: 4744837
Project duration: March, 2019 – September, 2019
Thesis committee:

Dr. ir. A. C. Schouten,	TU Delft
Dr. ir. W. Mugge,	TU Delft
Dr. L. Peternel,	TU Delft
Dr. P. A. Forbes,	Erasmus MC

An electronic version of this thesis is available at http://repository.tudelft.nl/.

TU Delft

CONTENTS

Modulation of stretch reflexes to environmental dynamics and perturbation properties

A. del Valle Hidalgo
Delft University of Technology, Delft, The Netherlands

September 16, 2019

Abstract

Reflexes and co-contraction are the two mechanisms used for effective limb control when humans face unexpected perturbations in their daily activities. When the environment has reduced stability margins, reflexes are tempered due to the oscillations caused by the neural time delay of the reflexive pathways. An explanation is that reflexes adapt to the dynamics of the environment and stability margins are the constraint. This view requires that humans assess stability margins, which could happen by detecting changes (i.e. oscillations) in the perturbation eliciting the reflexes. The perturbation perceived by the human is the actual perturbation filtered by the dynamics of the environment. Therefore, changes in the stability of the environment influence the perceived perturbation. The goal of this study is to determine whether reflex modulation is triggered by the environmental dynamics (i.e. damping and stability margins) or by the properties of the perturbation eliciting a reflexive response. An experiment was designed where participants were asked to minimize the displacements caused by continuous force perturbations applied to the hand while interacting with different environmental dynamics. Some of the perturbations were prefiltered to mimic the filtering effect of the environmental dynamics. Variations in the dynamics of the shoulder joint were quantified through the estimated arm admittance (i.e. displacements in response to force perturbations). The results show variations in the admittance between the perturbations mimicking the environment and the true environment at low frequencies (below 5Hz); and for different prior knowledge about the environmental dynamics (below 2Hz). These variations indicate that perturbations can be designed to mimic the environmental dynamics, and that perturbation properties and stability constraints cause changes in the motor behaviour.

***Index Terms*—Motor control, Reflex, Proprioception, Admittance, Afferent feedback, Stability, Perturbation design.**

I. Introduction

In daily-life, humans need to frequently interact with a wide variety of physical environments to perform activities such as holding a cup of tea while walking or keeping a screwdriver in the slot of a screw. Humans manage to successfully execute the intended tasks despite of the fact that the characteristics of these environments can significantly differ and perturbations may arise. Reflexes are one of the mechanisms, together with co-contraction (i.e. simultaneous activation of agonist and antagonist muscles), for effective limb control in the face of unexpected perturbations. However, patients suffering from Parkinson's Disease (Shadmehr and Krakauer, 2008; Mazzoni et al., 2012), post-stroke conditions (Finley et al., 2008; Meskers et al., 2009) or complex regional pain syndrome (Schouten et al., 2003; Mugge et al., 2012) present altered reflexes that disrupt the performance of these daily tasks; hence, the importance of studying the factors involved in the adaptability of reflexes.

Numerous studies focusing on stretch reflexes have proven that the task (Crago et al., 1976; Akazawa et al., 1983; Doemges and Rack, 1992b,a; Lewis et al., 2006; Abbink, 2007; Ludvig et al., 2007; Mugge et al., 2007; Perreault et al., 2008; Pruszynski et al., 2008, 2014; Pruszynski and Scott, 2012; Omrani et al., 2013), the frequency content of the perturbation eliciting the reflexes (Stein and Kearney, 1995; Kearney et al., 1997; Cathers et al., 1999; de Vlugt et al., 2001; van der Helm et al., 2002; Lewis et al., 2006; Mugge et al., 2007), the direction of the perturbation (Perreault et al., 2008; Pruszynski et al., 2008; Krutky et al., 2010), the amplitude of the perturbation (Stein and Kearney, 1995; Cathers et al., 1999; Weiler et al., 2016), and the dynamics of the environment (Milner and Cloutier, 1993; de Vlugt et al., 2002; Perreault et al., 2008; Finley et al., 2012), are factors of reflex adaptation.

One explanation for the adaptation to environmental dynamics is that reflexes contribute to the regulation of limb impedance (i.e. by increasing the joint stiffness) during postural control when the stability of the environment decreases (Perreault et al., 2008; Shemmell et al., 2009, 2010; Krutky et al., 2010). Another view is that reflexes are constrained by the stability margins of the environment in order to prevent the oscillations caused by the neural time delays of the reflexive pathways (Milner and Cloutier, 1993; de Vlugt et al., 2001, 2002; Finley et al., 2012). This idea was suggested by Milner and Cloutier (1993) after attaching the wrist to a manipulator with negative viscosity, so that the environment (i.e. the manipulator) removed the natural damping provided by the human. Under these conditions, the combined system (i.e. the human and the manipulator) was inherently unstable and increased levels of cocontraction, together with reduced reflexes, were required to limit large oscillations.

Despite these different views (Milner and Cloutier, 1993; de Vlugt et al., 2002; Perreault et al., 2008; Shemmell et al., 2010; Krutky et al., 2010) about the role of stability in reflex adaptation, all of them imply that humans are able to assess the stability of the environment. But how do we assess stability margins? One possible answer is by interacting with

the environment (i.e. system identification of the environment). Another one is that we detect changes in the characteristics of the perturbation (i.e oscillations at the point of interaction with the environment) eliciting the reflexes as these are filtered by the dynamics of the environment (Fig. 2). These dynamics influence the external perturbation designed for an experiment so that the actual perturbation we perceive (i.e. interaction signal between the human and the manipulator) is not the same as the external perturbation.

The goal of this study is to determine whether reflex modulation is triggered by the environmental dynamics (i.e. damping and stability margins) or by the properties of the perturbation eliciting a reflexive response. This can be formulated in a research question: 'What modulates stretch reflexes: environmental dynamics or perturbation properties?'

An experiment was designed to answer this question using a robotic manipulator. Participants were asked to minimize the displacements caused by continuous force perturbations (FP) applied to the hand while interacting with different environmental dynamics (i.e. several damping and therefore several stability margins). Some of the perturbations were prefiltered to mimic the filtering effect of the environmental dynamics (Fig.2). In this way, participants experience similar displacement profiles across different environments despite the underlying changes in the stability margins. For example, FPs mimicking a damped environment were applied in a no-damped environment. To go further in the study goal, we applied position perturbations (PP) with the displacements recorded in different environments. This also enable to study the influence of the perturbation type (PP/FP) in reflex modulation. Therefore, this study will examine if perturbations can be designed to mimic the environmental dynamics and if perturbation properties, in addition to stability constraints, are one of the factors of reflex modulation. These ideas are tested by quantifying variations in the dynamics through the estimation of admittance (i.e. displacements in response to force perturbations) of the shoulder joint, which is estimated as a function of frequency.

II. Methods

A. Participants

Fourteen right-handed male participants within an age range of 20-29 years, and without any relation with the study, participated in the experiment. All of them were self-reported to have no medical record of musculoskeletal or neurological disease, or injuries in the right arm. The experimental procedure was approved by the Human Research Ethics Committee of the Delft University of Technology.

From the fourteen participants, one of them performed just two-out-of-three repetitions due to a mechanical failure. Therefore, the experiment was not completed and this dataset was excluded.

B. Manipulator

The manipulator used to simulate the environments and apply the perturbations consists of a 1-degree-of-freedom linear electro-hydraulic actuator (Ruitenbeek JC and Janssen RJ, 1984) used in previous studies (de Vlugt et al., 2002; van der Helm et al., 2002; Schouten et al., 2008b; Forbes et al., 2011). Participants were seated upright in a chair (Fig.1) with adjustable height so that they could hold the handle of the manipulator with their right elbow flexed 90° and the lower arm aligned with the piston of the manipulator (reference position). In this way, displacements happened in the sagital plane with flexion/extension of the shoulder joint. A load cell (*31E-100N0*, Sensotec Instruments SA, Cornell de Llobregat, ES), placed between the handle and the piston, measured the force applied by the participants in the axis of motion. Position and velocity of the handle are measured as well.

The manipulator can be set in admittance mode or position mode. In the admittance mode (i.e. conditions with FP), the displacements of the handle are the result of the human reaction force, the force perturbation and the simulated environment (i.e. mass of 1kg, stiffness of 0 N/m and damping of 200 or 0 Ns/m). In the position mode (i.e. conditions with PP), the displacements are imposed by the manipulator regardless the reaction force of the participant. See Appendix A-A-Figure 10 for more details about the control scheme.

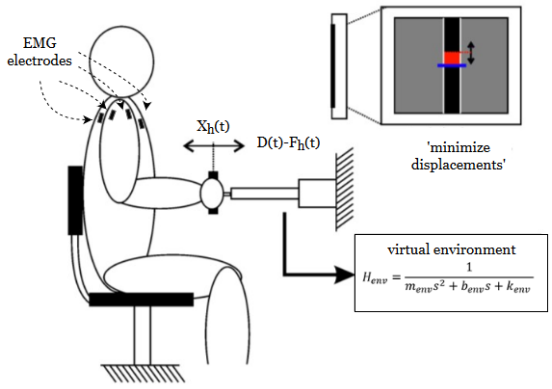

Fig. 1: Experimental set up. Participants are seated upright, holding the handle and minimizing the displacements of the handle while perturbations are applied. The position of the handle and the reference position are displayed on a screen. The environment simulated by the manipulator is modeled as a mass-spring-damper system. $F_h(t)$: force applied by the participant to the handle. $D(t)$ disturbance applied by the manipulator. $X_h(t)$ position of the handle. Four electrodes measure the EMG of the shoulder muscles.

C. Perturbation

We applied two types of perturbation (FP and PP) in two groups of conditions. In the original conditions, standard FPs were applied in a damped/no-damped environment to estimate the filtering effect of the environment. In the sham conditions, FPs mimicking the damped/no-damped environment were applied to the no-damped/damped environment, respectively. These FPs were generated using the displacement profiles of the original conditions. PPs were also applied in the sham conditions and were on-line generated from the displacements made by the participants during the original conditions.

The FP of the original conditions consisted of an odd random-phase multisine (Pintelon and Schoukens, 2012) with a fre-

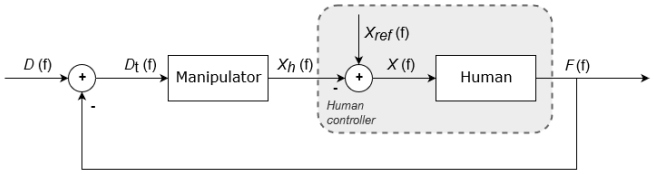

Fig. 2: Control scheme of the experimental set-up for posture control studies of the arm (van der Helm et al., 2002; Perreault et al., 2008) expressed in the frequency domain. An external force perturbation $D(f)$, together with the reaction force $F(f)$ of the human, forms a total force perturbation $D_t(f)$ that is input in the manipulator and transformed into displacements of the handle $X_h(f)$ to which the human is attached. Those displacements are the perturbation perceived by the human. As a response, the human generates a reaction force $F(f)$. The dotted rectangle represents the human controller performing a position task, where $X_{ref}(f)$ is the reference position.

quency bandwidth of 0.5-20 Hz (Fig. 3), which is sufficient to capture the dynamics of the arm (van der Helm et al., 2002). It was off-line generated with the fast-method: the odd harmonics were grouped in groups of three consecutive harmonics, randomly removing one of them in each group. All the harmonics had a constant power and the fundamental frequency was 0.125Hz (1/8s). The final FP was obtained from the repetition of 3 periods of the multisine (8s each) plus part of a fourth period to make 30s of perturbation.
The FPs of the sham conditions were on-line generated from the spectrum of the displacements recorded in the original conditions. The frequency content of the to-be-mimicked environment was scaled by the true environment. The generation of the perturbation followed three steps. For example, in the case of the sham conditions where the FP mimicked the damped while the true environment had no damping: first we derived the relation between the perturbation $D_{b0}(f)$ and the displacements of the handle $X_{b0}(f)$ during the original condition with the true environment (i.e no-damped environment):

$$\frac{X_{b0}}{D_{b0}} = \frac{H_{env\_b0}}{1 + H_{env\_b0}H_{h\_b0}} \tag{1}$$

Where H_{env_b0} and H_{h_b0} are the estimated frequency response functions (FRF) of the environment and of the human, respectively, for the no-damped environment ($b0$).

Second, we generated the new perturbation with the displacements of the handle during the original condition with the to-be-mimicked environment (i.e. $b200$: damped environment), and scaled them with the estimated FRF of the human and of the true environment (2). Regarding the estimated FRF of the human, there were two possibilities. One was using the estimated FRF of the human from the to-be-mimicked environment (H_{h_b0}), assuming that the human would response according to the environment mimicked by the perturbation. The other possibility was using the estimated FRF of the human from the true environment (H_{h_b200}) that the human would response according to the true environment. Both possibilities were tested.

$$D_{200x\_b0} = \frac{1 + H_{env\_b0}H_h}{H_{env\_b0}} X_{b200} \tag{2}$$

Where D_{200x_b0} is the FP of the sham condition generated from the displacements of the $b200$ condition applied in a true environment of $b0$.
Third, the final FP was obtained from the repetition of 3 periods of the new perturbation (D_{200x_b0}) plus part of a fourth period to make 30s of perturbation. This process is done for all the sham condition with FP (see Appendix A-B for more details about the process of generating perturbations).

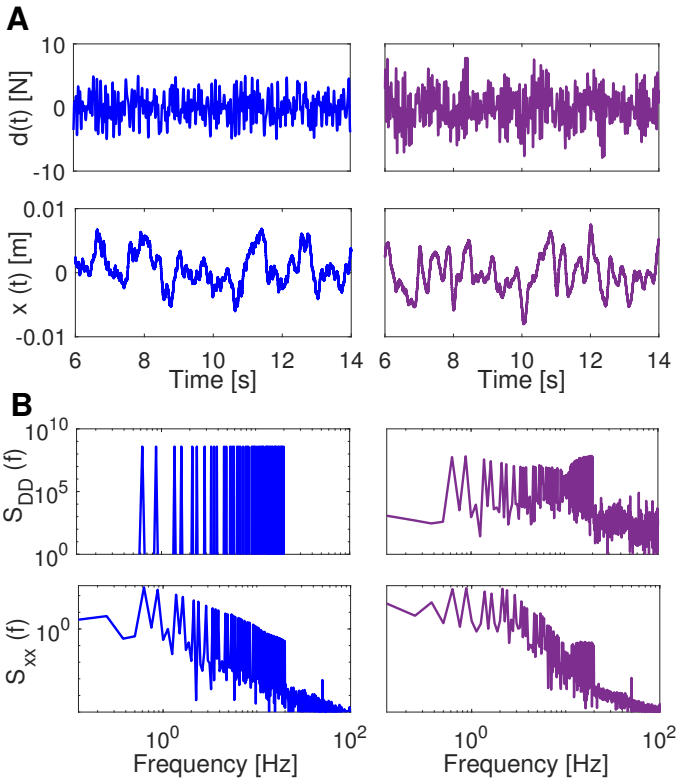

Fig. 3: Example of the filtering effect of the environmental dynamics on the external FP; and the resulting displacements of the hand for the $b200$ (*blue*) and $b200x\_0$ (*purple*) conditions. *A*: external FP $d(t)$ and displacements of the hand $x(t)$ in time domain. Only one-out-of-three periods are shown. *B*: power spectrum of the external FP $S_{DD}(f)$ and the displacements of the hand S_{XX}. The FP of the $b200$ condition has power at the excited harmonics only, while the FP of the $b200x\_0$ condition has power at non-excited harmonics as well. This power at non-excited harmonics is due to measurement noise and it was not removed during the perturbation generation to ensure the mimicking effect (see Appendix A-B).

D. Experimental protocol

Participants were asked to minimize the displacements around the reference position caused by continuous perturbations. There were two types of conditions. The original conditions (referred as $b200$, $b0$) consisted of standard FPs applied in a damped/no-damped environment (i.e. damping coefficients of 200 and 0 Ns/m respectively) to estimate the

filtering effect of the environment (H_{env}, H_h of equations 1-2). These conditions were applied first to get the displacements used to generate the perturbations of the sham conditions. The perturbations of the sham conditions mimicked the two environments of the original conditions (damped/ no-damped) while being applied in a different true environment (no-damped/damped). The FP perturbations were generated with the estimated FRF of the human, obtained from the original conditions, from either the true environment or the to-be-mimicked environment. This led to eight different experimental conditions: two original conditions, four sham conditions with FP (2 to-be-mimicked environments $\times$ 2 estimated FRF of the human), and two sham conditions with PP. These PP mimicked the two environments of the original conditions by reproducing the displacements.

In addition, an environment with damping of 0 or 200Ns/m, called the pre-trial environment (also referred as $bo0$ or $bo200$), was simulated before each trial and while participants were asked to move the handle to the reference position. For the original and sham conditions with PP, this pre-trial environment was the same as the to-be-mimicked environment. For the sham condition with FP, both types of environment (i.e. with damping of 0 or 200Ns/m) were uploaded to study the influence of prior knowledge in reflex adaptation. Therefore, the experiment consisted of a set of 12 trials, one for each condition of 30s each (Table I). This set was repeated three times. In the first two trials of every set, the original conditions were applied. Then the sham conditions were randomly applied. The perturbation of the sham conditions for each set were generated based on the original conditions of the same set. Participants had at least 30s of rest between trials and 3min of rest between repetitions. If needed, longer breaks were possible.

Participants trained with the original conditions before the actual experiment. During this training, the magnitude of the perturbations were adjusted to ensure equal handle displacements between participants and conditions. Those displacements were sufficiently small ($\pm$1cm from the reference position) to justify a linear model approximation (van der Helm et al., 2002; de Vlugt et al., 2002). Before and after the actual experiment, participants were asked to perform four force-task trials to establish the EMG-Force relationship through linear regression. They had to apply different levels of forces (-25, -20, -15, 0, 15, 20, 25N) while the handle was fixed. No perturbations were applied during these trials. After the experiment, the before- and after-experiment gains were compared to check that participants did not get muscle fatigue during the experiment.

E. Signal recording and processing

Position and velocity of the handle, the reaction force of the participant and the applied perturbation, were recorded. The electromyographic activity (EMG) of four shoulder muscles (pectoralis major, deltoids anterior, deltoids posterior and latissimus dorsi) was also recorded with bipolar surface electrodes (Hermens et al., 1999). The EMG signal of each muscle was conditioned with an amplification gain of 1000 and a band-pass filter of 20-450Hz (*Bagnoli EMG System*, Delsys, Natick, MA). Then, all signals were A/D converted with a sample frequency of 2.5kHz and 16 bits of resolution.

The EMG-force gains from the force-tasks were estimated with the procedure described by Schouten et al. (2008a). It consisted of a prewithening filtering followed by scaling and rectification. The parameters of the filter (6^{th} order) were obtained from the maximum force levels within the force-tasks. The gains for the pectoralis major and deltoids anterior are positive (i.e. push muscles) while for the latissimus dorsi and deltoids posterior (i.e. pull muscles) are negative, assuming that both muscles had equal relevance.

Initial and final transient effects were removed by excluding the first 4s and the last 2s of each trial in the processing. In addition, all signals were down sampled to 250Hz. For each experimental condition, all signals were divided in the three periods of a perturbation and transformed to the frequency domain with the fast Fourier transform and averaged over the three periods and over the three repetitions.

F. Non-parametric system identification

The admittance was estimated, for the frequencies excited by the multisine, to quantify the variations in the arm dynamics. It is related to the FRF of the human, relating the arm displacements to the input force. For the experimental conditions with FP, closed-loop system identification techniques ((van der Helm et al., 2002)) were used (3) because of the interaction between the participant and the manipulator (see Appendix A-A, Fig. 10):

$$\hat{H}_{XF}(f) = \frac{\hat{S}_{DX}(f)}{\hat{S}_{DF}(f)} \tag{3}$$

Where $\hat{H}_{FX}$ is the estimated admittance and $\hat{S}_{DX}$ and $\hat{S}_{DF}$ are the estimated cross-spectral densities between the designed perturbation D, the displacement of the handle X and the force F applied by the participant. To reduce the variance, all spectral densities were averaged over 2 adjacent frequencies.

For the experimental conditions with PP, there is no interaction between the manipulator and the participant. Therefore, open-loop techniques were used to estimate the admittance:

$$\hat{H}_{FX}(f) = \frac{\hat{S}_{XX}(f)}{\hat{S}_{XF}(f)} \tag{4}$$

To evaluate the linear assumption based on small displacements, we estimated the coherence γ^2. It indicates if two signals are linearly related and free of noise, ranging from 0 to 1 (linear system without noise). For the experimental conditions with FP, coherence was estimated with closed-loop system identification techniques:

$$\hat{\gamma}^2_{DX}(f) = \frac{|\,\hat{S}_{DX}(f)\,|^2}{\hat{S}_{DD}(f)\hat{S}_{XX}(f)} \tag{5}$$

For the experimental conditions with PP, open-loop techniques were used:

$$\hat{\gamma}^2_{XF}(f) = \frac{|\,\hat{S}_{XF}(f)\,|^2}{\hat{S}_{FF}(f)\hat{S}_{XX}(f)} \tag{6}$$

TABLE I: Experimental matrix. The sham conditions with FPs are named according to the structure: '*b:to-be-mimicked environment__true-environment__h: estimated-human-FRF__bo:pretrial-environment*', where the environment is defined by the damping coefficient.

Experimental condition	To-be-mimicked Env. (Ns/m)	True Env. (Ns/m)	H_{human}	Pretrial Env. (Ns/m)
$b0$	0	0	-	0
$b200$	200	200	-	200
$b200x\_0\_h0\_bo0$	200	0	0	0
$b0x\_200\_h0\_bo0$	0	200	0	0
$b200x\_0\_h200\_bo0$	200	0	200	0
$b0x\_200\_h200\_bo0$	0	200	200	0
$b0\_pp$	0	PP	0	-
$b200\_pp$	200	PP	200	-
$b200x\_0\_h0\_bo200$	200	0	0	200
$b0x\_200\_h0\_bo200$	0	200	0	200
$b200x\_0\_h200\_bo200$	200	0	200	200
$b0x\_200\_h200\_bo200$	0	200	200	200

G. Statistical analysis

The influence of the pretrial environment and the estimated FRF of the human used to generated the FP was evaluated with a three-way repeated-measures ANOVA on the magnitude of the estimated admittance. The experimental variables used for this ANOVA were: the to-be-mimicked environment, the pretrial environment and the estimated FRF of the human used to generate the FP perturbations of the sham conditions (Table II).

The mimicking effect of the sham conditions and the effect of the type of perturbation were evaluated with multiple comparisons using the post-hoc Bonferroni test. This test uses the results from a one-way repeated-measures ANOVA performed on the magnitude of the estimated admittance of the conditions $b0$, $b200$, $b0pp$, $b200pp$, $b0x\_200\_h0\_bo0$ and $b200x\_0\_h0\_bo0$. The last two conditions were selected from the group of conditions with the same to-be-mimicked environment, but different FRF of the human and pretrial environment (i.e. $b0x\_200\_h200\_bo0$, $b0x\_200\_h200\_bo200$, $b0x\_200\_h0\_bo200$, $b0x\_200\_h0\_bo0$ and $b200x\_0\_$...). These two conditions were considered to be representative of the sham conditions with the same to-be-mimicked environment (i.e. $b0x$ and $b200x$). In this way, we avoided statistical power loss due to grouping and a possible influence of the FRF of the human or of the pre-trial environment because those were the same for both conditions. In addition,

TABLE II: 3D matrix with the experimental conditions evaluated in the three-way ANOVA. The number in brackets refer to the third dimension (i.e. the to-be-mimicked environment). *(1)*: $b0x\_200$ conditions. *(2)*: $b200x\_0$ conditions.

		Estimated FRF of the Human	
		H_{h0}	H_{h200}
Pretrial Environment	bo_0	b0x_200_h0_bo0(1) b200x_0_h0_bo0(2)	b0x_200_h200_bo0(1) b200x_0_h200_bo0(2)
	bo_200	b0x_200_h0_bo200(1) b200x_0_h0_bo200(2)	b0x_200_h200_bo200(1) b200x_0_h200_bo200(2)

the pretrial and the true environment were identical, as it is the case of the other conditions tested (i.e. the original and sham conditions with PP).

Both ANOVAs were applied at frequencies below 5Hz, where changes in the admittance are expected (de Vlugt et al., 2002). These frequencies were grouped in two. Namely, Group 1 with frequencies between 0.5Hz and 2Hz, and Group 2 with frequencies between 2Hz and 5Hz. For each group, a group-admittance was calculated by taking the average of the admittance over the frequency points included in the group. estimated. The ANOVAs were applied twice, one for each frequency group, with a level of significance of $p<0.05$.
Previous to these analyses, the distribution of the data was evaluated with a Chi-square goodness-of-fit test to ensure a normal distribution, as assumed by the ANOVA.

III. Results

The Chi-square goodness-of-fit test, with a significant level of 0.01, did not reject the null hypothesis. This hypothesis was that the magnitude of the admittance followed a normal distribution over the participants for all experimental conditions and for both frequency groups.

A. Mimicking perturbations and resultant displacements

The perturbation of the sham conditions presented peaks/dips between 2 and 5Hz when mimicking the no-damped/damped environment (Fig. 4A). These features compensated for the filtering effect of dynamics of the environment. The FRF of a no-damped environment presents an oscillation peak around its resonance frequency. Therefore, the perturbation must compensate this oscillation with a dip in the spectral density when the to-be-mimicked environment is damped and the true environment is no-damped ($b200x\_0\_...$ and $b200pp$ conditions). The opposite applies when mimicking a no-damped environment. The perturbation presents a peak in the spectral density ($b0x\_200\_...$ and $b0pp$ conditions) to generate the oscillations caused by a no-damped environment and prevented by the damping of the true damped environment. The perturbations of the sham conditions that differ just in the pretrial environment are the same. This is because the pretrial environment does not influence the process of generating the perturbations.
On closer inspection of the estimated power spectrum of the resultant displacements (Fig. 4B-C), we observe similar power distributions, in terms of shape, between the original and the sham conditions. The power spectrum of the sham conditions with PP and the original conditions are the same, as expected. This equality is due to the process of generation the perturbation (i.e. the PP were generated from the power spectrum of the displacements of the original conditions).

B. Non-parametric system identification

The response of the participants was consistent among the repetitions. This was proven by the small standard deviation

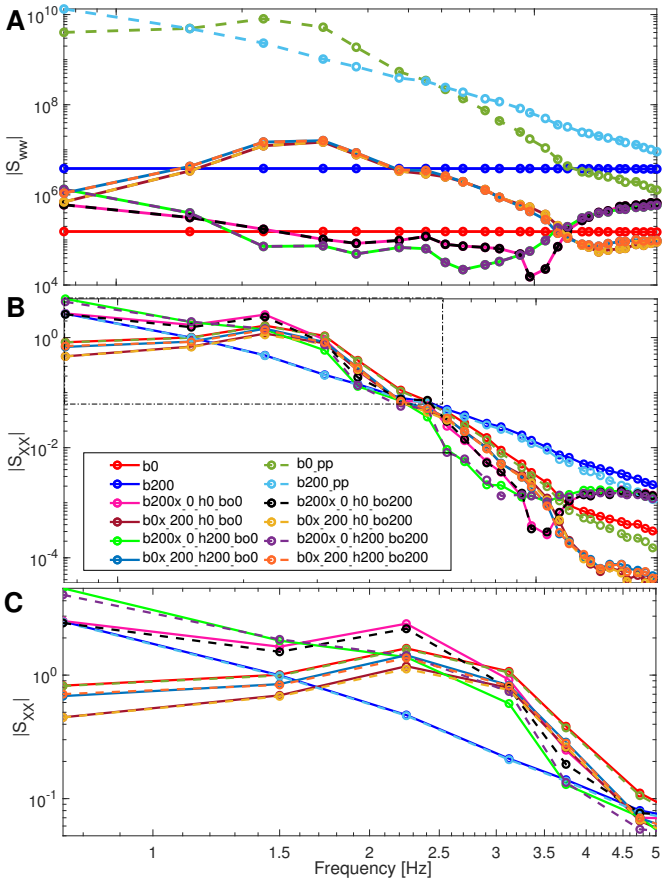

Fig. 4: Average power spectrum of the perturbations applied to one of the participants (*A*) and of the resultant displacements (*B*). The power spectrum of the displacement is zoomed in on the middle and low frequencies (*C*). The solid and dashed lines represent the original and sham conditions, respectively.

of the spectrum of the measurements (Fig. 5). The averaged admittances of all participants were similar, as expected, among the experimental conditions at frequencies above 5Hz (Appendix B - Fig. 11). Therefore, the statistical analysis was performed for frequencies below 5Hz (Fig. 6) in the two groups described in Section II-G.
The high coherence (above 0.75) for all experimental conditions indicates a linear behaviour, justifying the linear approach, with low levels of noise (Appendix B- Fig. 11). There is an exception for the condition $b200\_pp$, where the coherence drops to 0.6 around 3Hz. Nevertheless, all values are above the significant level (0.2209).

C. Influence of the pretrial environment and the estimated FRF of the human

From the results of the three-way repeated-measures ANOVA (Table III), we did not find a significant difference in the magnitude of the estimated admittance at middle frequencies (Group 2: $2-5Hz$) when comparing experimental conditions with different estimated human FRF. We did find a significant difference at low frequencies (Group 1: $0.5-2Hz$). Therefore, the estimated FRF of the human used to generated a FP for the sham condition had an influence on the low

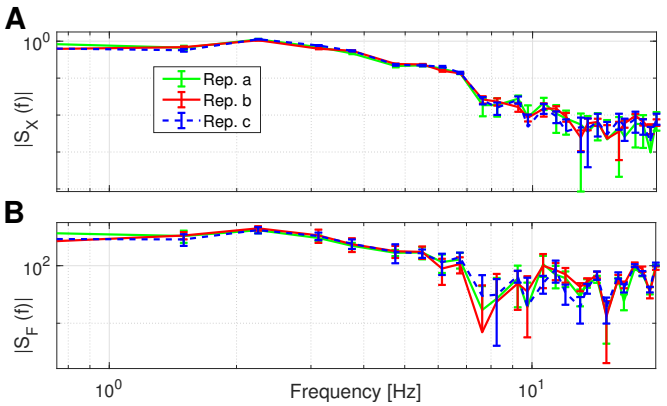

Fig. 5: Spectrum of force (*A*) and displacement (*B*) measured for one condition over the three repetitions (a-c) from one of the participants.

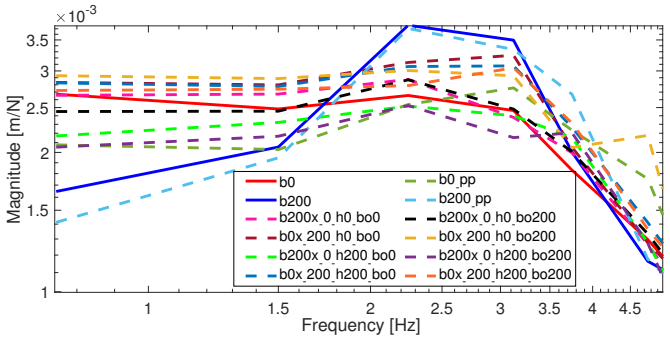

Fig. 6: Average admittance over participants of all the experimental conditions zoomed in on the middle and low frequencies.

frequencies of the admittance (Fig. 7).
When looking at the pretrial environment, we found similar results. Namely, there were significant differences at low frequencies but not at middle frequencies. This indicates that the pretrial environment had an influence on the low frequencies of the admittance.
Furthermore, we found a significant influence of the to-be-mimicked environment for both frequency groups.
No significant interaction was found between these three experimental variables. This means that the experimental variables (to-be-mimicked environment, pretrial environment and estimated FRF of the human) were not significantly interdependent. As a consequence, the mimicking effect of the sham conditions with the FP could be evaluated using the one-way ANOVA with just two-out-of-eight of the with-FP sham conditions (i.e. $b0x\_200\_h0\_bo0$ and $b200x\_0\_h0\_bo0$ representing the $b0x\_200\_...$ and $b200x\_0\_...$ conditions), as described in Section II-G.

D. Mimicking effect of the perturbations

The one-way repeated measures ANOVA found that there were significant differences ($p < 0.0001$) among the experimental conditions tested. The multiple comparisons (Table IV) showed that the magnitude of the admittance of original conditions was significantly different for both group of frequencies, as expected (Fig. 8).

TABLE III: P-values from the three-way repeated measures ANOVA. bo: pretrial environment. bx: to-be-mimicked environment. H_h: estimated FRF of human. The last four rows refer to the interaction between these experimental variables.

	Group1 $(0.5-2Hz)$	Group2 $(2-5Hz)$
H_h	0.0041	0.5844
bo	0.0498	0.9082
bx	<0.0001	0.0231
$H_h - bo$	0.6547	0.3419
$H_h - bx$	0.1553	0.9900
$bo - bx$	0.2611	0.6508
$bo - bx - H_h$	0.3818	0.4132

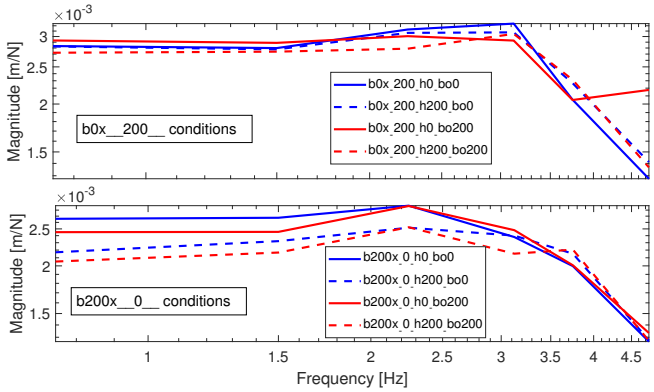

Fig. 7: Comparison of the average admittance of experimental conditions with different pretrial environments (*blue lines*: bo_0; *red lines*: bo_200) and different estimated FRFs of the human (*solid lines*: h_0; *dashed lines*: h_200).

Comparing the with-FP sham condition mimicking the damped environment (i.e. $b200x\_0\_h0\_bo0$) with the original conditions (i.e. $b0$ and $b200$), no significant differences were found at any of the frequency groups except for the middle frequencies and between the sham condition and the $b200$ condition. Regarding the with-FPs sham condition mimicking the no-damped environment (i.e. $b0x\_200\_h0\_bo0$), significant differences were found with respect to the $b200$ condition at all frequencies.
In the case of the sham conditions with PPs, there were significant differences between the sham condition $b0\_pp$ and the original condition $b0$ at low frequencies, and between the $b0\_pp$ and the original condition $b200$ at middle frequencies. Regarding the $b200\_pp$ condition, there was a significant difference with the original condition $b0$ at all frequencies.

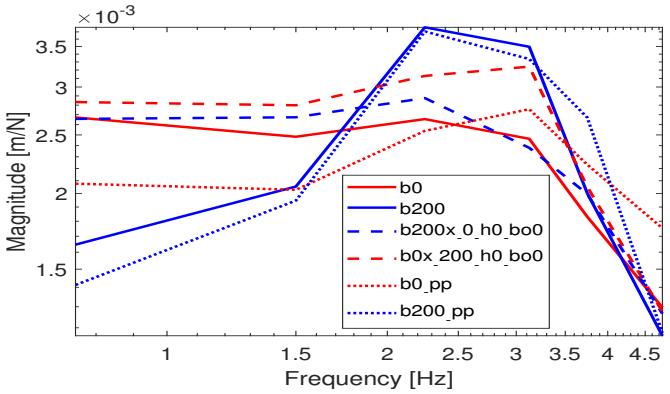

Fig. 8: Comparison of the average admittance between the original conditions (*solid lines*), the sham conditions with FP (*dashed lines*), and the sham conditions with PP (*dotted lines*).

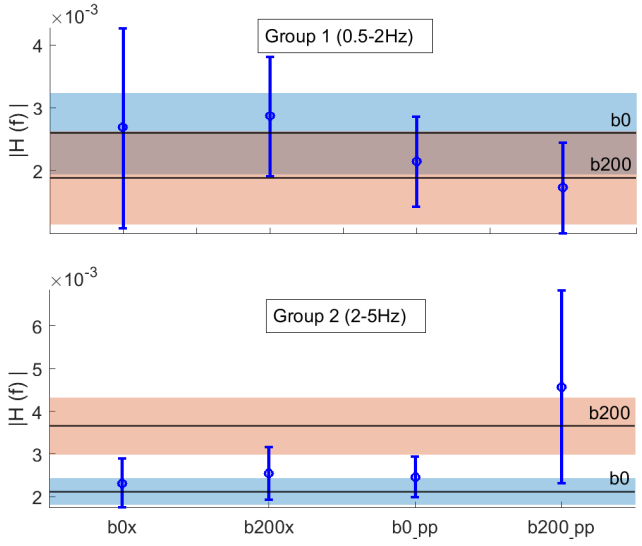

Fig. 9: Mean and standard deviation of the admittance of the experimental conditions tested in the one-way repeated measures ANOVA. The shaded areas represent the standard deviation of the original conditions (*blue*: $b0$; *red*: $b200$), and the horizontal lines their means.

E. Influence of the type of perturbation

The influence of the type of perturbation was evaluated from the results of the one-way ANOVA (Table IV) by comparing the sham conditions with FP ($b0x\_200$, $b200x\_0$), with the equivalent sham conditions with PP ($b0pp$, $b200pp$). No significant differences were found at middle frequencies. In contrast, significant differences were observed at low frequencies between the $b200x$ and the $b200\_pp$ conditions, and between the $b0x$ and the $b0\_pp$ conditions.

IV. Discussion

A. Pretrial environment and estimated FRF of the human influence the admittance

That the pretrial environment influenced the arm admittance at low frequencies (Fig. 7) indicates that participants responded to the perturbation according to their prior knowledge about the dynamics of the environment. The influence of the situation previous to the elicitation of reflexes has already been suggested by Pruszynski and Scott (2012) when discussing about the effect of the behavioral context on reflexes. In addition, Koshland and Hasan (2000) observed that perturbations applied just before a reaching movement resulted in the activation of the muscles involved in that movement during the reflexive response, even when the perturbation did not affect them. And Lewis et al. (2006) observed that the task-dependent modulation of reflexes was due to an early release of the intended movement, similar to what Ravichandran et al. (2013) proved with startle reflexes.

The FRF of the human used to generated the FP for the sham conditions also influenced the admittance at low frequencies. Therefore, the assumptions made about the human response (i.e. reflexes adapt to the true environment or to the to-be-mimicked environment) affect the actual response. Conse-

TABLE IV: P-values from the multiple comparisons of the one-way repeated measures ANOVA. $b0x$ and $b200$ refer to the sham conditions $b0x\_200\_h0\_bo0$ and $b200x\_0\_h0\_bo0$, respectively.

Compared conditions		Group1 $(0.5-2Hz)$	Group2 $(2-5Hz)$
b0	b200	<0.0001	<0.0001
b200x	b0	1	0.5266
b200x	b200	0.1260	0.0002
b200x	b0x	1	0.6413
b200x	b0pp	1	1
b200x	b200pp	0.0488	0.0606
b0x	b0	0.7553	0.0817
b0x	b200	0.0004	0.0034
b0x	b0pp	0.0015	1
b0x	b200pp	<0.0001	0.1078
b0pp	b0	0.0158	0.0696
b0pp	b200	0.8629	0.0003
b0pp	b200pp	0.0095	0.0757
b200pp	b200	1	1
b200pp	b0	<0.0001	0.0313

quently, the design of future studies should consider carefully which assumptions are made about the human response before generating the mimicking perturbations; and what information (i.e. pretrial environment) is provided to the participants before the actual trial.

B. Perturbation properties influence the admittance

The admittances of the original conditions were significantly different, which means that different environments (damped/no-damped) cause variations in the arm dynamics through co-contraction and reflexes. This was already proven by de Vlugt et al. (2002) and Perreault et al. (2008).

The admittance of the with-FP sham condition mimicking the no-damped environment, when the true environment was damped, was different to the admittance of the original condition with the same true environment (i.e. damped). The same effect was observed in the case of the with-PP sham condition mimicking the damped environment. Therefore, these perturbations successfully mimicked the no-damped/damped environment when the actual environment was damped/no-damped. The rest of the sham conditions caused in-between effects (Fig. 8-9). The admittance at low frequencies of the with-FP sham condition mimicking the damped environment was not different to either of the original conditions (i.e. damped/no-damped environment), which were indeed different between them (Fig. 9). And the admittance of the PP mimicking the no-damped environment was different to the no-damped environment at low frequencies, and to the damped one at middle frequencies. Consequently, the dynamics of the environment are not the only factor of changes in the admittance, and the properties of the perturbation influence on the admittance as well.

Variations in the admittance represent changes in the motor behaviour of the participants that can be due to different levels of co-contraction or to different reflex gains (van der Helm et al., 2002). Previous studies (de Vlugt et al., 2002; Perreault et al., 2008) proved that reflex gains are modulated to the dynamics of the environment. Indeed, de Vlugt et al. (2002) proved that reflexes are different when interacting with a damped environment (200 Ns/m) than with a no-damped (0 Ns/m) environment. Because the environments used by de Vlugt et al. are the same as the ones used in this study, we assume that the variations in admittance observed in this study are also caused by variations in the reflex gains, as de Vlugt et al. proved. Therefore, reflexes are likely to be modulated both to the dynamics of the environment and to the perturbation properties. This suggests that stability margins are not the only cause of reflex modulation.

C. The type of perturbation might not influence the admittance

The difference in admittance found at low frequencies of the with-PP and with-FP sham conditions mimicking the no-damped environment is explained by the difference with respect the original condition. The admittance of the PP was different to that of original condition with the no-damped environment. However, the admittances of the FP and the no-damped environment were not different. Therefore, the difference in admittance between the type of perturbation was likely to be caused by the unsuccessful mimicking effect of the PP at low frequencies. No diffirence was found at middle frequencies or between the with-PP and with-FP sham conditions mimicking the damped environment. The lack of influence of the type of perturbation was also observed by (Forbes et al., 2011) when studying the reflexive contribution to posture maintenance during EMG tasks.

V. Conclusion

This study addresses the influence of the dynamics of the environment on the perturbation perceived by the human and on the reflexes elicited. Variations in the arm dynamics (admittance) are not solely caused by changes of the dynamics of the environment (stability margins), but also by the properties of the perturbation. This study also shows that perturbations can be designed to mimic the dynamics of the environment and that the prior knowledge about those dynamics can affect the later motor behaviour.

References

Abbink, D. A. (2007). Task instruction: The largest influence on human operator motion control dynamics. In *Proceedings - Second Joint EuroHaptics Conference and Symposium on Haptic Interfaces for Virtual Environment and Teleoperator Systems, World Haptics 2007*, pages 206–211.

Akazawa, K., Milner, T. E., and Stein, R. B. (1983). Modulation of reflex EMG and stiffness in response to stretch of human finger muscle. *Journal of Neurophysiology*, 49(1):16–27.

Cathers, I., O'Dwyer, N., and Neilson, P. (1999). Dependence of stretch reflexes on amplitude and bandwidth of stretch in human wrist muscle. *Experimental Brain Research*, 129(2):278–287.

Crago, P. E., Houk, J. C., and Hasan, Z. (1976). Regulatory Actions of Human Stretch Reflex. *Journal of Neurophysiology*, 39(5):925–935.

de Vlugt, E., Schouten, A. C., and van der Helm, F. C. (2002). Adaptation of reflexive feedback during arm posture to different environments. *Biological Cybernetics*, 87:10–26.

de Vlugt, E., van der Helm, F. C., Schouten, A. C., and Brouwn, G. G. (2001). Analysis of the reflexive feedback control loop during posture maintenance. *Biological Cybernetics*, 84:133–141.

Doemges, F. and Rack, P. M. (1992a). Changes in the stretch reflex of the human first dorsal interosseous muscle during different tasks. *The Journal of Physiology*.

Doemges, F. and Rack, P. M. (1992b). Task-dependent changes in the response of human wrist joints to mechanical disturbance. *Journal of Physiology*, 447:575–585.

Finley, J. M., Dhaher, Y. Y., and Perreault, E. J. (2012). Contributions of feed-forward and feedback strategies at the human ankle during control of unstable loads. *Experimental Brain Research*, 217:53–66.

Finley, J. M., Perreault, E. J., and Dhaher, Y. Y. (2008). Stretch reflex coupling between the hip and knee: Implications for impaired gait following stroke. *Experimental Brain Research*, 188(4):529–540.

Forbes, P., van der Helm, F. C., and Schouten, A. C. (2011). EMG feedback tasks reduce reflexive stiffness during force and position perturbations. *Experimental Brain Research*, 213:49–61.

Hermens, H. J., Freriks, B., Merletti, R., Stegeman, D., Blok, J., Rau, G., Disselhorst-Klug, C., and Hägg, G. (1999). European Recommendations for Surface ElectroMyoGraphy Results of the SENIAM project. *Roessingh research and development*, 8(2):13–54.

Kearney, R. E., Stein, R. B., and Parameswaran, L. (1997). Identification of intrinsic and reflex contributions to human ankle stiffness dynamics. *IEEE Transactions on Biomedical Engineering*, 44(6):493–504.

Koshland, G. F. and Hasan, Z. (2000). Electromyographic responses to a mechanical perturbation applied during impending arm movements in different directions: one-joint and two-joint conditions. *Exp Brain Res*, 132(4):485–499.

Krutky, M. A., Ravichandran, V. J., Trumbower, R. D., and Perreault, E. J. (2010). Interactions Between Limb and Environmental Mechanics Influence Stretch Reflex Sensitivity in the Human Arm. *Journal of Neurophysiology*, 103:429–440.

Lewis, G., MacKinnon, C. D., and Perreault, E. J. (2006). The effect of task instruction on the excitability of spinal and supraspinal reflex pathways projecting to the biceps muscle. *Experimental Brain Research*, 174(3):413–425.

Ludvig, D., Cathers, I., and Kearney, R. E. (2007). Voluntary modulation of human stretch reflexes. *Experimental Brain Research*, 183(2):201–213.

Mazzoni, P., Shabbott, B., and Cortés, J. C. (2012). Motor Control Abnormalities in Parkinson's Disease. *Cold Spring Harb Perspect Med.*, 2(6).

Meskers, C. G., Schouten, A. C., De Groot, J. H., De Vlugt, E., Van Hilten, B. J., Van Der Helm, F. C., and Arendzen, H. J. (2009). Muscle weakness and lack of reflex gain adaptation predominate during post-stroke posture control of the wrist. *Journal of NeuroEngineering and Rehabilitation*, 6(1):29.

Milner, T. E. and Cloutier, C. (1993). Compensation for mechanically unstable loading in voluntary wrist movement. *Experimental Brain Research*, 94(3):522–532.

Mugge, W., Abbink, D. A., and Van Der Helm, F. C. (2007). Reduced power method: How to evoke low-bandwidth behaviour while estimating full-bandwidth dynamics. In *2007 IEEE 10th International Conference on Rehabilitation Robotics, ICORR'07*, pages 575–581.

Mugge, W., Munts, A. G., Schouten, A. C., and van der Helm, F. C. (2012). Modeling movement disorders-CRPS-related dystonia explained by abnormal proprioceptive reflexes. *Journal of Biomechanics*, 45(1):90–98.

Omrani, M., Diedrichsen, J., and Scott, S. H. (2013). Rapid feedback corrections during a bimanual postural task. *Journal of Neurophysiology*, 109(1):147–161.

Perreault, E. J., Chen, K., Trumbower, R. D., and Lewis, G. (2008). Interactions With Compliant Loads Alter Stretch Reflex Gains But Not Intermuscular Coordination. *Journal of Neurophysiology*, 99(5):2101–2113.

Pintelon, R. and Schoukens, J. (2012). *System Identification: A Frequency Domain Approach, Second Edition*. John Wiley and Sons.

Pruszynski, J. A., Kurtzer, I., and Scott, S. H. (2008). Rapid Motor Responses Are Appropriately Tuned to the Metrics of a Visuospatial Task. *Journal of Neurophysiology*, 100(1):224–38.

Pruszynski, J. A., Omrani, M., and Scott, S. H. (2014). Goal-Dependent Modulation of Fast Feedback Responses in Primary Motor Cortex. *Journal of Neuroscience*, 34(13):4608–17.

Pruszynski, J. A. and Scott, S. H. (2012). Optimal feedback control and the long-latency stretch response. *Experimental Brain Research*, 218(3):341–59.

Ravichandran, V. J., Honeycutt, C. F., Shemmell, J., and Perreault, E. J. (2013). Instruction-dependent modulation of the long-latency stretch reflex is associated with indicators of startle. *Experimental brain research*, 230(1):59–69.

Ruitenbeek JC and Janssen RJ (1984). Computer-controlled manipulator display system for human-movement science. *Med Biol Eng*, 22:304–308.

Schouten, A., de Vlugt, E., and Van der Helm, F. (2008a). Design of perturbation signals for the estimation of proprioceptive reflexes. *IEEE Trans Biomed Eng*, 55:1612–1619.

Schouten, A. C., De Vlugt, E., Van Hilten, J. J., and Van Der Helm, F. C. (2008b). Quantifying proprioceptive reflexes during position control of the human arm. *IEEE Transactions on Biomedical Engineering*, 55(1):311–321.

Schouten, A. C., Van de Beek, W. J. T., van Hilten, J., and van der Helm, F. C. (2003). Proprioceptive reflexes in patients with reflex sympathetic dystrophy. *Experimental Brain Research*, 151(1):1–8.

Shadmehr, R. and Krakauer, J. W. (2008). A computational neuroanatomy for motor control. *Experimental Brain Research*, 185(3):359–381.

Shemmell, J., An, J. H., and Perreault, E. J. (2009). The Differential Role of Motor Cortex in Stretch Reflex Modulation Induced by Changes in Environmental Mechanics and Verbal Instruction. *Journal of Neuroscience*, 29(42):13255–13263.

Shemmell, J., Krutky, M. A., and Perreault, E. J. (2010). Stretch sensitive reflexes as an adaptive mechanism for maintaining limb stability. *Clinical Neurophysiology*, 121(10):1680–1689.

Stein, R. B. and Kearney, R. E. (1995). Nonlinear behavior of muscle reflexes at the human ankle joint. *Journal of Neurophysiology*, 73(1):65–72.

van der Helm, F. C., Schouten, A. C., de Vlugt, E., and Brouwn, G. G. (2002). Identification of intrinsic and reflexive components of human arm dynamics during postural control. *Journal of Neuroscience Methods*, 119:1–14.

Weiler, J., Saravanamuttu, J., Gribble, P. L., and Pruszynski, J. A. (2016). Coordinating long-latency stretch responses across the shoulder, elbow, and wrist during goal-directed reaching. *Journal of Neurophysiology*, 116(5):2236–2249.

APPENDIX A
PERTURBATION GENERATION

This appendix provides more details about the generation of the perturbations applied in the experiment. First it proves that any of the measurements provided by the manipulator (position, velocity and force) can be used to generate new perturbations with identical results. Then, it describes the steps taken to generate the perturbations of the sham conditions.

A. Equivalence of perturbations generated from force, position or velocity measurements

The manipulator enables the measurement of the force applied by the participants to the handle as well as the position and velocity of the handle (Fig.10). The present study uses the displacements measured in the original conditions to generate the perturbation for all the sham conditions, as described in Section II-C:

$$\frac{X(s)}{D(s)} = \frac{H_{env}(s)}{1 + H_{env}(s)H_h(s)} \tag{7}$$

$$D(s) = \frac{1 + H_{env}(s)H_h(s)}{H_{env}(s)} X(s) \tag{8}$$

Where $D(s)$ is the spectrum of a FP for the sham conditions; H_{env} is the FRF of the true environment that was estimated from the original conditions; H_h is the estimated FRF of the human; and $X(s)$ is the spectrum of the displacements from the original condition whose environment is to be mimicked.

Other option to generate the perturbation is using the velocity measured in the original conditions:

$$\frac{\dot{X}(s)}{D(s)} = \frac{sH_{env}(s)}{1 + H_{env}(s)H_h(s)} \tag{9}$$

$$D(s) = \frac{1 + H_{env}(s)H_h(s)}{sH_{env}(s)} \dot{X}(s) \tag{10}$$

However, considering the relation between position and velocity ($\dot{X}(s) = sX(s)$), we reach the same result as using the displacements (8):

$$D(s) = \frac{1 + H_{env}(s)H_h(s)}{sH_{env}(s)} sX(s) = \frac{1 + H_{env}(s)H_h(s)}{H_{env}(s)} X(s) \tag{11}$$

A third option to generate the perturbation is using the measured force (12). However, considering the relation between position and force ($F(s) = H_h(s)X(s)$) we reach the same result as using the measured displacements (8):

$$\frac{F(s)}{D(s)} = \frac{H_{env}(s)H_h(s)}{1 + H_{env}(s)H_h(s)} \tag{12}$$

$$D(s) = \frac{1 + H_{env}(s)H_h(s)}{H_{env}(s)H_h(s)} F(s) = \frac{1 + H_{env}(s)H_h(s)}{H_{env(s)}} X(s) \tag{13}$$

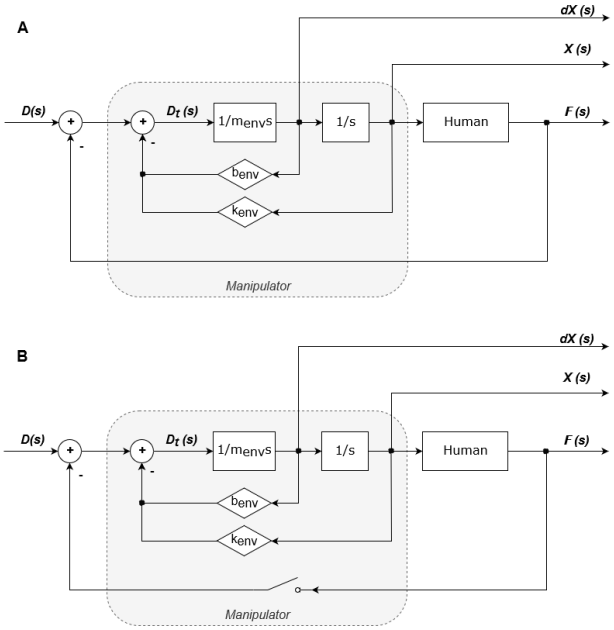

Fig. 10: Control scheme of the manipulator in the frequency domain. $D(s)$: designed disturbance. $D_t(s)$: total disturbance input to the manipulator. $X(s)$: position of the handle. $dX(s)$: velocity of the handle. $F(s)$: force applied by the participant to the handle. m_{env}: mass of the simulated environment. b_{env}: damping of the simulated environment. k_{env}: stiffness of the simulated environment. In the admittance mode (A), the manipulator is force controlled and the simulated environment had a mass, damping and stiffness of 0kg, 0 or 200 N/ms, and 0 N/m, respectively. In the position mode (B), the manipulator is position controlled and the simulated environment had a mass, damping and stiffness of 0kg, 800 N/ms, and 70,000 N/m, respectively.

B. Generation of perturbation for the sham conditions

The perturbations for the sham conditions were generated from the displacement measured during the original conditions:

1) Force perturbations: the perturbations were generated based on the spectrum of the displacements recorded during both of the original conditions, following the next steps:

1) Selection of 24s of the recorded data from the original conditions, removing the first 4s and the last 2s to discard transient any effect.

2) Split of the data in 3 segments, according to the three periods (8s each) of the multisine FP.
3) Transformation of the data to the frequency domain using the Fast Fourier Transform (FFT) for each segment.
4) Averaging over the segments.
5) Estimation of the transfer functions of the human and the environment.
6) Calculation of the spectrum of one period of the mimicking perturbation according to Equation 8 and the experimental condition (i.e. to-be-mimicked environment, true environment and FRF of the human).
7) Transformation of the spectrum of the period to the time domain using the inverse FFT.
8) Removal of any offset introduced in the process.
9) Down-sampling of the period from 2500Hz to 312.5Hz and filtering with an anti-aliasing filter.
10) Repetition of the period three times and part of a fourth one to make 30s of perturbation.
11) Multiplication of the resultant perturbation by ascending/descending ramps of 0.38s at the beginning/end, respectively, to guarantee safe start/end of the trial.

2) Position perturbation: the perturbations were generated based on the displacements recorded during the original conditions.

1) Selection of the displacements from the original condition whose environment was the same as the to-be-mimicked environment.
2) Down-sampling of the 30s-displacement from 2500Hz to 312.5Hz and filtering with an anti-aliasing filter.
3) Multiplication of the displacements by ascending/descending ramps of 0.64s at the beginning/end, respectively, to guarantee safe start/end of the trial.

Due the measurement noise, the spectrum of the recorded displacement had power at frequencies non-excited by the perturbation of the original condition (i.e multisine). These power was not removed during the generation of the perturbation of the sham conditions because the power of the excited harmonics was clearly higher than the one of the non-excited harmonics (Fig. 3). In addition, that would have added power to the excited frequencies so that the mimicking effect could have been ineffective.

APPENDIX B
DETAILS OF STATISTICAL ANALYSIS

This appendix provides more details about the averaged admittance of each experimental condition. It also provides the MATLAB code used to perform the statistical analysis, and the distribution of the admittances used for it.

A. MATLAB code used for the statistical analysis

```

%%%%%%%%%%%%%%%%%%%%%%  3-way ANOVA %%%%%%%%%%%%%%%%%%%%%%
% Experimental variables:
% Bx:to-be-mimicked env.
% bo: pretrial env.
% h:FRF of human
varNames=cell(2*2*2,1);
% Conditions 3:6,9:12 of TABLE I are assigned the name c1:8
for ii=1:length(varNames)
    varNames{ii,1}=strcat('c',num2str((ii)));
end
Hrepmeas=[squeeze((Hall(k,[3:6 9:12],:)))]'; % Magnitude of admittance of condition 3:6, 9:12 of TABLE I
trepmeas=array2table(Hrepmeas,'VariableNames',varNames');

%Values of the experimental variables:
Var1=[{'b200x'} {'b0x'} {'b200x'} {'b0x'} {'b200x'} {'b0x'} {'b200x'} {'b0x'} ];
Var2= [{'h0'},{'h0'},{'h200'},{'h200'},{'h0'},{'h0'},{'h200'},{'h200'}]';
Var3=[{'bo0'},{'bo0'},{'bo0'},{'bo0'},{'bo200'},{'bo200'},{'bo200'},{'bo200'}]';
Vartable=[Var1 Var2 Var3 ];
trepmeas_var=array2table(Vartable,'VariableNames',[{'bx'},{'h'},{'bo'}]);

%repeated measures model
rm=fitrm(trepmeas,'c1-c8~1','WithinDesign',trepmeas_var)

% mean and  std of the selected admittances by exp. variable
ranova_mc_bx_h_bo_stats=grpstats(rm,{'bx', 'bo','h'})

% repeated measures anova
ranova_bx_h_bo=ranova(rm,'WithinModel','bx*h*bo');

ranova_mc_h_bx=multcompare(rm,'h','By','bx','ComparisonType','bonferroni');
ranova_mc_bx_bo=multcompare(rm,'bo','By','bx','ComparisonType','bonferroni')
ranova_mc_h_bo=multcompare(rm,'h','By','bo','ComparisonType','bonferroni')


%%%%%%%%%%%%%%%%%%%%%%% 1-way ANOVA %%%%%%%%%%%%%%%%%%%%%%
 varNames=[];
% Conditions 1:4, 7:8 of TABLE I are assigned the name c1:6
Hrepmeas_bx=[squeeze(Hall(k,[1 2 3 4 7 8],:))]'; % Magnitude of admittance of conditions of TABLE I


trepmeas_bx=array2table(Hrepmeas_bx,'VariableNames',{'c1' 'c2' 'c3' 'c4' 'c5' 'c6'});
trepmeas_bx_var=array2table({'b0'; 'b200'; 'b0x'; 'b200x' ;'b0pp' ;'b200pp'  },'VariableNames',{'bx'});

%repeated measures model
rm=fitrm(trepmeas_bx,'c1-c6~1','WithinDesign',trepmeas_bx_var)

% mean and std of the selected admittances
ranova_mc_bx_stats=grpstats(rm,{'bx'})

% repeated measures anova
ranova_bx=ranova(rm)


%multiple comparisons with bonferroni correction
ranova_mc_bx=multcompare(rm,'bx','ComparisonType','bonferroni') %
```

B. Averaged admittance and coherence

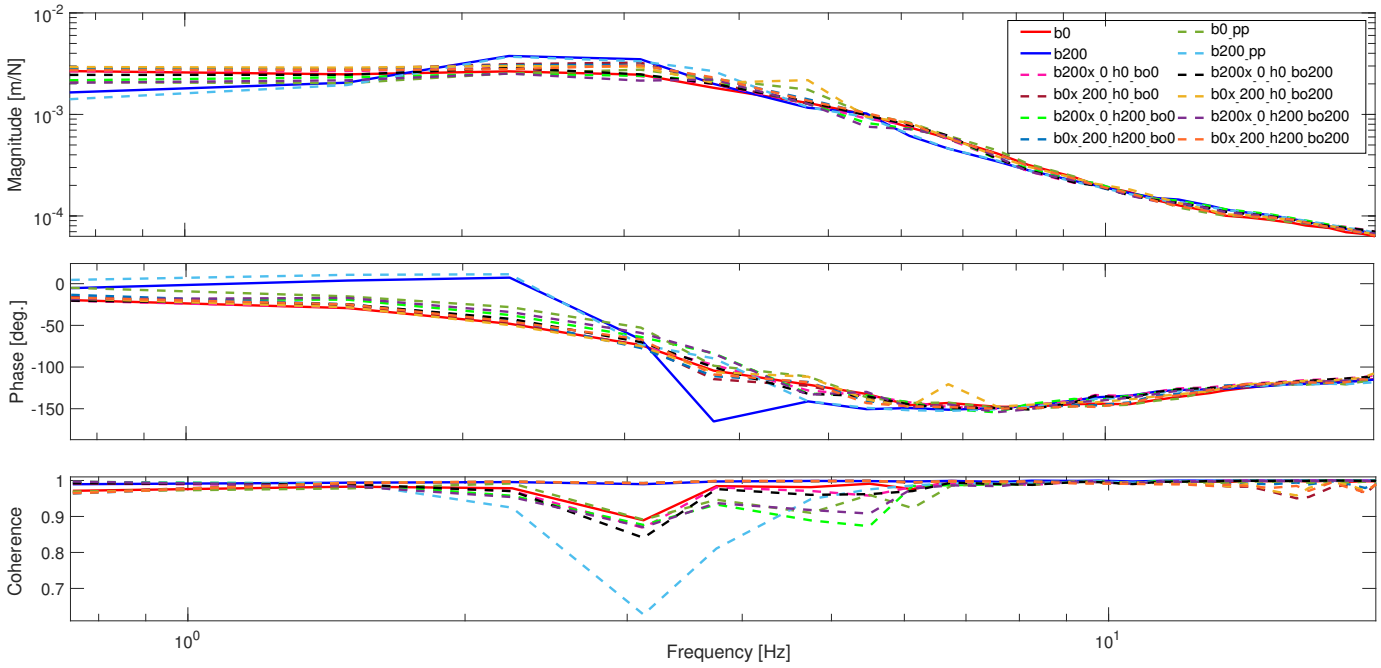

Fig. 11: Average admittance (magnitude and phase) and coherence over the participants of all the experimental conditions.

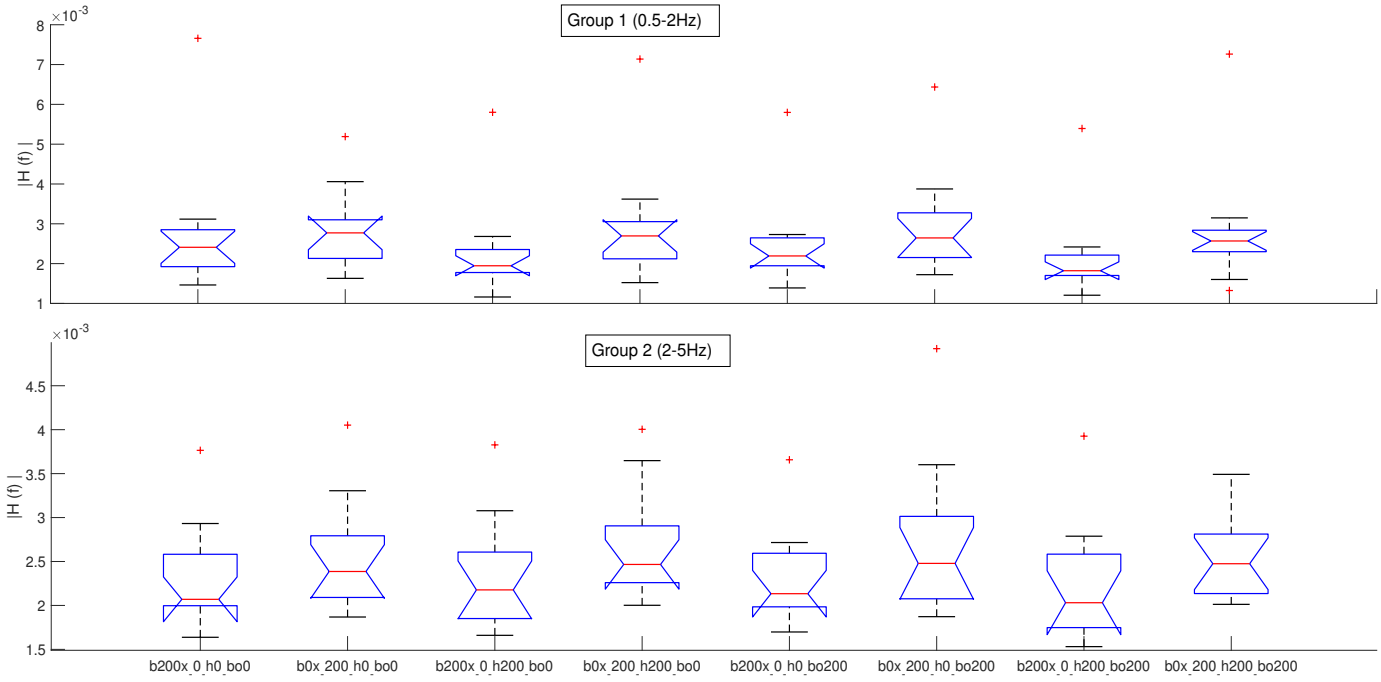

Fig. 12: Box-plot of the magnitude of the admittance of the experimental conditions evaluated with the three-way ANOVA for each frequency group.

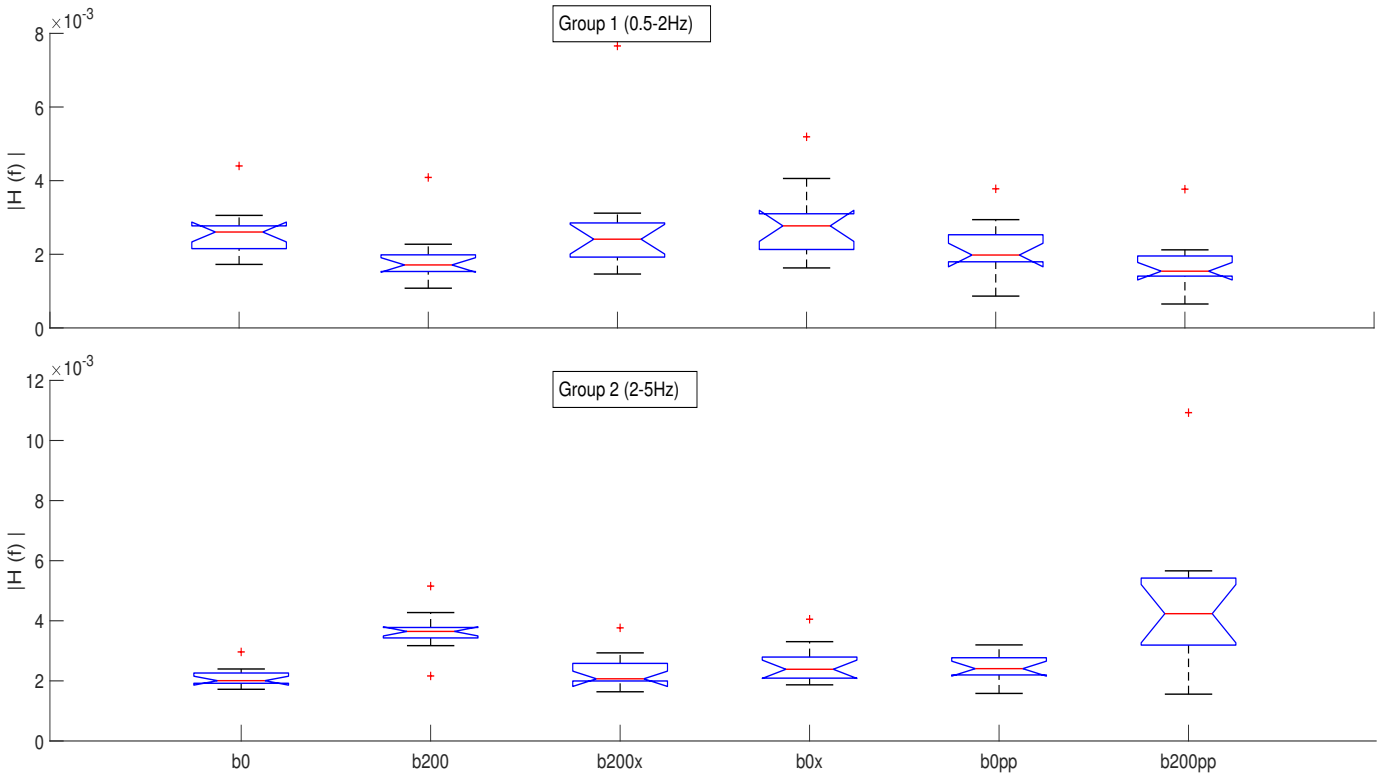

Fig. 13: Box-plot of the magnitude of the admittance of the experimental conditions evaluated with the one-way ANOVA for each frequency group.